

## HETERO-JUNCTION MODULE TECHNOLOGY

M. Späth<sup>1\*</sup>, D. Veldman<sup>1</sup>, N. Dekker<sup>1</sup>, I. Bennett<sup>1</sup>, W. Eerenstein<sup>1</sup>, P.C. de Jong<sup>1</sup>, P.J. Ribeyron<sup>2</sup>, S. Harrison<sup>2</sup>, D Muñoz<sup>2</sup>

<sup>1</sup>ECN Solar Energy, P.O. Box 1, 1755 ZG Petten, The Netherlands

<sup>2</sup>INES-CEA, Savoie Technolac - 50 avenue du lac Léman - BP258 F-73375 Le Bourget-du Lac, France

\*Corresponding author: Phone: +31 224 564828; Fax: +31 224 568214; email: spath@ecn.nl

**ABSTRACT:** Silicon hetero-junction solar cell technology has the potential to obtain high efficiencies with thin wafers. Cell efficiencies of 21 % can be achieved on 170 micron thin wafers. A significant reduction of the cost-performance ratio can be realized if these fragile cells are integrated reliably in solar modules. This requires low stress and low-temperature interconnection of individual cells. Also, hetero-junction cells are known to be susceptible to moisture ingress inside the module. Single cell modules have been manufactured using conductive adhesive as interconnection and using a moisture blocking back sheet to protect the cells. The modules have been exposed to climate chamber tests (damp-heat and thermal cycling) according to the IEC 61215 ed. 2 standard. Infrared analysis (IR) and electroluminescence (EL) images were taken to investigate the integrity of cells and their interconnections. Modules made with moisture blocking back-sheets showed that the modules did survive 1500 hours (1.5 times IEC) of damp heat and over 340 thermal cycles with less than 5% reduction in power output. The industrial feasibility of this module technology was demonstrated by manufacturing 72-cell modules, using cells obtained from an industrial party. Assembly of the modules was done using a tabber-stringer capable to work with conductive adhesives, designed for low temperature interconnection.

**KEYWORDS:** Hetero-junction, interconnection, reliability testing.

### 1 INTRODUCTION

In standard H-pattern modules, solar cells are interconnected by soldering tabs. This process is done at temperatures well in excess of 250°C, which will have a detrimental effect on the performance and mechanical yield of thin hetero-junction cells. Hetero-junction cells [1] contain a thin, amorphous Si layer and a TCO layer on top of the Si wafer. The passivated amorphous Si layer cannot withstand temperatures in excess of 200°C. Furthermore, the TCO layer is moisture sensitive. This means hetero-junction cells cannot be placed in modules using the same components and materials as used for manufacturing standard H-pattern modules, i.e. with (lead-) tin containing solders and TPT back sheets.

ECN's module technology consists of an interconnection method based on conductive adhesives. The use of conductive adhesives in conjunction with low-temperature silver metallization on the cell is a fundamentally different technology and raises concern in terms of electrical resistivity and reliability. The stability of the interconnection between cell metallization and conductive adhesive is a very critical parameter. Both depend on the thermo mechanical properties and moisture stability of many different components.

This paper describes the results of two projects, i.e., the EU-FP7 project HETSI and an industrial project. Reliability tests were conducted on 125x125mm<sup>2</sup> pseudo-square mono crystalline silicon hetero-junction cells manufactured at INES-CEA with a cell thickness of 170 µm and cell efficiencies up to 19%. At ECN a novel module design was developed to achieve long-term stable modules for these solar cells. The module design focused on low stress interconnect, moisture blocking and optical optimization of the hetero-junction modules. In addition, cell-to-module losses were determined for a 72 cell module containing industrially manufactured hetero-junction cells.

### 2 EXPERIMENTAL SET UP

The low-temperature processes employed in making hetero-junction solar cells imply that the electrical conductivity of both front-side and rear-side metallization on the cell is not as good as for conventional solar cells using high-temperature fired-through metallization. This could also affect the cell to module losses.

To confirm whether this is the case, cells with two types of screen-printable silver paste were manufactured and the series respectively the contact resistance were investigated. The metallization screen print material was either a low-temperature silver polymer or an industrial high-temperature silver paste. The low-temperature metallization was cured at < 200°C while the standard cell paste was fired at a temperature just above 850°C. Electrical resistivity targets have been formulated in the HETSI project in order to realize hetero-junction cells with an efficiency of at least 19% [2] and minimizing the efficiency loss of 1% absolute on module level.

Four cell modules (2x2) were manufactured incorporating conductive adhesive as interconnection medium. The electrical performance of cells and module were compared and losses determined by analyzing the IV characteristics.

Single cell modules were made with one module having a standard TPT back sheet (reference module) and the other modules comprising a moisture blocking back sheet. Five mini-modules were tested in damp heat, up to 1500 hours (1.5xIEC) and five were tested in thermal cycle, up to 345 cycles (1.7xIEC).

The 72 cell module, 6x12 configuration and cell size 125x125 mm<sup>2</sup> on semi-square wafers, was manufactured at a specially designed tabber stringer at ECN. The interconnection material of choice was conductive adhesive.

### 3 RESULTS AND DISCUSSION

#### 3.1 Resistance properties for high and low temperature silver metallization pastes

Samples containing low-temperature silver metallization paste were compared to samples with “standard” high-temperature (“fired”) metallization silver paste. The tab-to-tab resistance (RTT), i.e. series resistance over the bus-bar was determined by measuring the resistance between two tabs attached to the front bus-bar of the cell (see Fig. 1). Resistance measurements were performed based on the four-wire method.

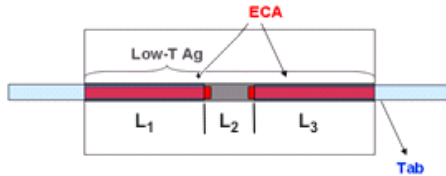


**Figure 1:** Schematic of the samples used for tab-to-tab resistance measurements. The arrows indicate the locations of contacting. ECA denotes electrical conductive adhesive.

Two silver plated copper tabs were adhered to a bus-bar consisting of low-temperature silver paste. Two different samples (LowT1 and LowT2) were used in combination with electrical conductive adhesive (ECA). A Si wafer covered with ITO was used as a substrate. In addition two silver plated copper tabs were adhered to a bus-bar consisting of fired high-temperature silver paste (HighT1 and HighT2) using conductive adhesive. A Si wafer covered with SiNx was used as a substrate. After dispensing the CA on the substrates, the tabs were adhered and cured. Afterwards, the substrates were sandwiched between a sheet of ethyl vinyl acetate (EVA) and glass on the front side and a sheet of EVA and TPT foil in the rear side. The tabs were guided through an opening in the TPT foil. Finally, the samples were laminated at 150° C for 15 minutes.

RTT [mΩ] can be described as a series resistance of the bus-bar over the length  $l_2$  (Fig. 1) a parallel resistance over the tab, conductive adhesive and the bus-bar over the lengths  $l_1$  and  $l_3$ :

$$RTT = \left( \frac{1}{R_{tab}} + \frac{1}{R_{CA}} + \frac{1}{R_{Ag}} \right)^{-1} (l_1 + l_3) + R_{c(tab-CA)} + R_{c(CA-Ag)} + R_{Ag} l_2$$

With  $R_{tab}$ ,  $R_{CA}$  and  $R_{Ag}$  denoting the line resistivities (Ω/m) of the tab, the conductive adhesive and the silver paste of the bus-bar.  $R_{c(tab-CA)}$  is the contact resistances between tab and conductive adhesive.  $R_{c(CA-Ag)}$  between conductive adhesive and silver paste, respectively.

Samples HighT1 and HighT2 with conventional high-temperature silver paste result in  $RTT = 29 \pm 3$  mΩ. From the line resistance of the bus-bar prior to adhesion of the tabs ( $R_{Ag} = 12.6$  Ω/m) and using  $l_2 = l_3$  [cm], we find  $R_{Ag} l_2 = 17$  mΩ.

For the samples with low-temperature silver paste a RTT value of  $85 \pm 1$  mΩ is measured. The major part (80-95%) of this resistance can be explained by the line resistance of the bus-bar ( $R_{Ag} = 73 \pm 10$  mΩ/cm for the central section). Thus the very high RTT value is mainly

caused by the high bulk resistance of the low-temperature silver paste. Note that RTT is still nearly three times higher than that of the samples with the high-temperature silver paste. RTT is dominated by the line resistance of the low temperature silver material. Here the line resistance is more than 5 times higher compared to the High T samples.

#### 3.2 Cell to module resistance

The transmission line model (TLM) can be used to determine the specific contact resistance between two materials. Here, TLM is used to determine the specific resistance ( $\rho_c$ ) of the contact area between a silver plated copper tab and a low-temperature silver paste bus-bar that is adhered with dots of conductive adhesive (CA). The result of the TLM measurements will present a value for the sum of the contact resistance between the conductive adhesive and the tab ( $\rho_{c,CA-Tab}$ ), the conductive adhesive and the silver paste ( $\rho_{c,CA-Ag}$ ) and finally the bulk resistivity of the conductive adhesive. In the following sections the sample preparation and results are described.

For the TLM measurements, Si wafers covered with ITO were used as substrates. Silver plated copper tabs were adhered to the bus-bar consisting of low temperature silver paste using CA. The tabs were placed perpendicular to the bus bar at distances increasing from 1 to 5 silver fingers (Fig. 2). After adhering the tabs by curing with infrared lamps on the tabber stringer, the samples were laminated between glass and TPT foil using EVA.



**Figure 2:** Sample prepared for TLM measurement

The specific contact resistance can be determined from a plot of the resistance, measured between two consecutive tabs using 4-wire resistance measurements, versus the distance between these tabs. The value at which a linear fit crosses the y-axis (at a distance of  $x = 0$ ) is the resistance corresponding to two contact areas. Therefore the specific contact resistance  $\rho_c$  can be determined from the following formula:

$$\rho_c = R(x=0)/2 \cdot A$$

with  $R(x=0)$  the resistance at a distance of  $x = 0$  determined from the crossing with the y-axis and the surface area [A] of the contact (here  $2.7 \times 2.7$  mm<sup>2</sup>).

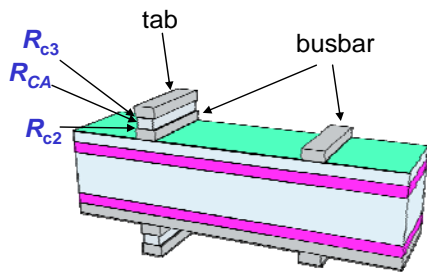


**Figure 3:** Cross section of cell and interconnection

The results of TLM measurements revealed the sum of contact resistances. Starting from the bus-bar up to the conductive adhesive  $R_{c2}$  and from conductive adhesive to the tab  $R_{c3}$  (see Fig. 3) the contact resistance amounts to  $\rho c = 0.1 \text{ m}\Omega \text{ cm}^2$ . This is equivalent to a series resistance of  $0,11 \text{ m}\Omega$  per cell. The bulk resistivity of the conductive adhesive ( $R_{CA}$ ) is in the order of  $5 \cdot 10^{-4} \Omega \text{ m}$  which is  $0.15 \text{ m}\Omega$  per cell. For the tab a bulk resistivity of  $2 \cdot 10^{-8} \Omega \text{ m}$  was measured to be a series resistance of  $2.33 \text{ m}\Omega$  per cell. These results show that the series resistance of the tab is 15 times higher than the series resistance of the conductive adhesive. Therefore, the series resistance of the conductive adhesive is not the dominating factor. Interconnect losses as a result of applying conductive adhesives are of less importance.

### 3.4. Reliability tests

Reliability tests have been conducted on single cell modules by performing damp heat and thermal cycle according to IEC61215 ed. 2 and beyond. Damp heat testing was extended to 1500 hours and thermal cycle testing was stopped after 345 cycles. Previous experiments indicated that the hetero-junction cells are prone to humidity. Preventing degradation was anticipated by adding a protection layer to the back-sheet, see Fig. 4.

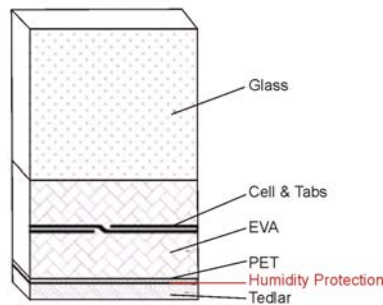


**Figure 4:** Cross section of module containing hetero-junction cells, conductive adhesive interconnection and humidity protected back-sheet.

#### 3.4.1 Damp heat testing

Damp-heat testing showed that the module with added humidity protection easily passed 1000 hours of damp-heat testing. Some of these modules survived up to 1500 hours of damp-heat exposure. The modules showed

a power loss of 2.3%, 4.0%, 5.6% and respectively 2 modules with 6 % of original power. The observed degradation of the modules can be attributed to the loss in short-circuit current. The fill factor losses are less significant. This indicates that the interconnection with conductive adhesives is more stable than the cell itself. If cell degradation could be prevented, the modules would only show limited degradation. The observed cell degradation is likely to be caused by moisture ingress through the edges of the module. Sufficient edge sealing should thus prevent the cell degradation observed here. Humidity as a cause of cell degradation was evident as one module comprised a standard TPT back sheet for reference purposes. This module showed severe cell degradation during the first 500 hours of damp heat testing.

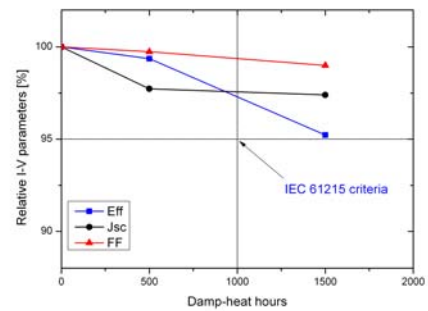


**Figure 5:** All modules have been made with a humidity blocking back-sheet. Note that the efficiency, Jsc and FF are an average of the 5 modules mentioned. Eff denotes module efficiency as a function of DH exposure. Jsc the short circuit current and FF the fill factor as a function of DH exposure.

#### 3.4.2 Thermal Cycle testing

The purpose of thermal cycling is to determine the ability of the module to withstand thermo mechanical stresses caused by repeated changes of temperature.

A total of 5 single cell modules were subjected to temperature cycling. A total of 345 thermal cycles did not lead to a significant degradation of the modules and the results are fair within the 5% power limit dictated by the IEC61215 protocol.

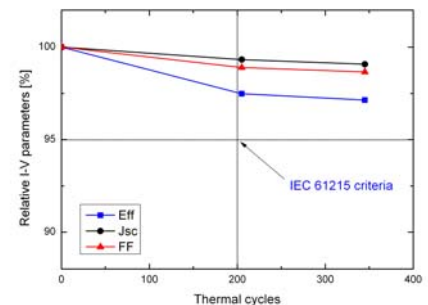


**Figure 6:** Results of climatic chamber testing of 5 modules containing hetero-junction cells. Degradation was normalized to 100% of original output power.

### 3.5 Optical loss from cell to module for single cell modules

Besides electrical losses, optical losses can occur in a module as well. Optical losses in the module exist by light absorption and/or reflection of light due to interference of light waves through the layers of material in front of the hetero junction cell, and light reflected back from the cell. The module materials in front of the cell are the glass plate and the EVA encapsulant. Light which passes through these layers hits the TCO layer, then the amorphous Si layer and can then enter the Si wafer, where each absorbed photon can create one electron-hole pair. At each interface described above, light can be reflected and in each layer, absorption of light can take place. Optical losses in this hetero-junction configuration have been modeled and it was found that by using extra thin EVA (200  $\mu\text{m}$ ) and glass with an anti-reflection coating, 0.36% absolute efficiency gain can be achieved compared to a hetero-junction module with standard thickness EVA (400  $\mu\text{m}$ ) and non coated glass.

This was tested by comparing single cell modules using standard glass and EVA thickness, and single cell modules with thin EVA and AR coated glass. The measured increase in performance of the modules with thin EVA and AR coated glass was 0.26% absolute. This is 0.1% less than calculated, the difference might be explained by the fact that the optical loss model does not take the texture of the amorphous- Si and TCO surface into account, resulting in a larger effect on efficiency.

### 3.6 Manufacturing of 72 cell hetero-junction modules

A module with 72 industrially supplied hetero-junction cells was constructed, see Fig. 7. Assembly of the modules was done with the aid of the ECN tabber-stringer installation. From a manufacturing point of view the assembling went well as the structural integrity of the cells has been of high quality. Breakage of the cells did not occur during interconnection and fast introduction of elevated curing temperatures.

The measured performance was compared against simulated expectations. The module performance is in close agreement to simulated results.

Input parameters for the simulation were measured from the hetero-junction cells directly, such as the resistances of the bus-bar, fingers and TCO layers. In addition, TLM measurements were carried out to obtain resistance numbers of the conductive adhesive interconnections.



**Figure 7:** Hetero-junction module with 72 cells, manufactured at the ECN tabber stringer using conductive adhesive.

## 5 CONCLUSIONS

Hetero-junction modules have been successfully manufactured using conductive adhesive as interconnect method. The series resistance between the bus-bar of the hetero-junction cell and the conductive adhesive and up to the tab including conductive adhesive does not have any significant impact on the module fill factor. The tab series resistance is dominating the interconnection being 15 times higher than the series resistance of the conductive adhesive. The stability of the interconnections also proved to be good for thermal cycling with a power loss of only 2.5% during extended testing. The loss in power output after damp heat reached the 5% limit according to IEC61215 after an extended test duration of 1.5 times IEC, i.e. 1500 hrs. Damp heat testing showed that the interconnection with conductive adhesives remains stable, but the cell itself can show degradation hetero-junction cells appears to be the most critical component with respect to moisture ingress. Standard TPT back sheet does not block moisture ingress sufficiently for module manufacturing when using these cells. Additional care must be taken with the edge sealing of the module to prevent moisture ingress. Large scale modules containing 72 cells were also manufactured showing our interconnection method to be industrially feasible.

### Acknowledgements

This work was partly conducted within the FP7 Integrated Project HETSI and funded by the European Commission under contract nr. 211821.

### References

- [1] W.G.J.H.M. van Sark, L. Korte, F. Roca (Eds.) Physics and technology of amorphous-crystalline heterostructure silicon solar cells, Springer Verlag, Heidelberg, Germany, 2011, 580 pages.
- [2] P.J. Ribeyron et al, Results of the HETSI project. Published at this conference.